

# **Response to the SSC PAC**

## **BCD Collaboration**

(July 11, 1990)

### **Executive Summary**

This Response is divided into six sections corresponding to the six questions posed to the BCD Collaboration by the SSC PAC. The text of these questions is reproduced at the beginning of each section.



# Contents

<b>1</b>	<b>Comparison of <math>B</math>-Physics Options</b>	<b>1</b>
1.1	$B$ -Physics Opportunities at Hadron and $e^+e^-$ Colliders . . . . .	1
1.2	$B$ Physics with Hadron Accelerators . . . . .	4
1.2.1	Comparison of the BCD and SFT (SSC-EOI0014) . . . . .	5
1.3	$B$ Physics in Other Collider Experiments . . . . .	7
1.3.1	SSC: BCD and SDC . . . . .	7
1.3.2	TEV I: Mini-BCD and CDF . . . . .	7
1.4	Non- $B$ Physics at the BCD . . . . .	12
<b>2</b>	<b>Doing <math>B</math> Physics at a Hadron Collider</b>	<b>13</b>
2.1	$B$ -Meson Signals at CDF . . . . .	13
2.2	Vertexing Efficiency . . . . .	14
2.3	Tracking Efficiency . . . . .	18
2.4	Effect of Multiple Interactions . . . . .	19
2.5	Efficiency of Particle Identification . . . . .	21
<b>3</b>	<b>BCD at Very High Luminosity</b>	<b>22</b>
<b>4</b>	<b>Sensitivity to CKM Angle <math>\varphi_3</math> Via <math>B_s</math> Decays</b>	<b>22</b>
4.1	Tagging with Kaons . . . . .	23
<b>5</b>	<b>Alternative Detector Configurations and Staging</b>	<b>25</b>
5.1	Alternative Detector Configurations . . . . .	25
5.2	Staging . . . . .	27
<b>6</b>	<b>Funding in FY91</b>	<b>28</b>
<b>7</b>	<b>References</b>	<b>30</b>

# List of Tables

1	Sensitivity of the BCD to $\sin 2\varphi_1$ . . . . .	1
2	Sensitivity of an asymmetric $e^+e^-$ collider to $\sin 2\varphi_1$ . . . . .	3
3	Sensitivity of an asymmetric $e^+e^-$ collider to $\sin 2\varphi_2$ . . . . .	3
4	$B-\bar{B}$ production at hadron accelerators . . . . .	4
5	Geometric acceptance for single $B$ decays. . . . .	8
6	Rate estimates for reconstructed $B$ decays. . . . .	9
7	Geometric acceptance for tagging $B$ decays. . . . .	10
8	Acceptance for tagged $B$ decays. . . . .	10
9	Rate estimates for tagged, reconstructed $B$ decays. . . . .	11
10	Efficiency of the kaon tag . . . . .	24
11	List of detector subsystems . . . . .	26
12	Broad-based alternative detector configurations . . . . .	27

## List of Figures

1	Vertex efficiency <i>vs.</i> $P_t$ cut . . . . .	14
2	Silicon detector resolution <i>vs.</i> angle of incidence . . . . .	15
3	Error in the vertex reconstruction . . . . .	16
4	Distance from primary to secondary vertex . . . . .	17
5	$P_t$ cut for the vertex reconstruction . . . . .	18
6	The closest-distance-of-approach cut . . . . .	19
7	The $S/\delta S$ cut on secondary vertices . . . . .	20
8	Mass spectrum of 'fake' vertices in $B$ events . . . . .	20
9	Mass spectrum of 'fake' vertices in $D$ events . . . . .	21

# 1 Comparison of $B$ -Physics Options

To BCD from R.F. Schwitters, June 12, 1990:

1. Aiming at a deeper discussion of the issues raised after your presentation on June 8, would you please expand on the following points:

- How do you compare the potential of BCD to that of an  $e^+e^-$  asymmetric  $B$ -factory at the  $\Upsilon(4S)$  with a luminosity of  $10^{33}$ , and  $10^{34} \text{ cm}^{-2}\text{sec}^{-1}$ ?
- Given the apparent large difference in cost between the BCD project and a fixed target experiment, how would you defend the collider option in terms of physics advantages?
- What part of the BCD physics program could be carried out by a general purpose large detector (e.g., SDC)?
- Are there other domains of application of the BCD detector in addition to  $B$ -physics?

## 1.1 $B$ -Physics Opportunities at Hadron and $e^+e^-$ Colliders

The projected sensitivity of the BCD at the SSC to the interior angles of the CKM unitarity triangle is given in Table 1.

Table 1: Update of Table 11 of the BCD EOI to include a Kaon tag. The minimum values of  $\sin 2\varphi_i$  resolvable to three standard deviations in  $10^7$  sec of running at luminosity of  $10^{32} \text{ cm}^{-2}\text{sec}^{-1}$ . The factor  $1 - 2p$  is the analyzing power of the tag which has a probability  $p$  for a wrong tag.  $b$  is the background to signal for the final-state reconstruction. The dilution factor  $D$  due to mixing is given by  $x_q \coth(\pi/2x_q)/(1 + x_q^2)$ .

Angle	Mode	Tag	Tagged Events	$1 - 2p$	$b$	$x_q$	$D$	$\sin 2\varphi_{\min, 3\sigma}$
$\varphi_1$	$B_d^0 \rightarrow J/\psi K_S^0$	$e^\pm$	14,400	0.60	0.1	0.7	0.47	0.094
$\varphi_1$	$B_d^0 \rightarrow J/\psi K_S^0$	$K^\pm$	110,000	0.40	0.1	0.7	0.47	0.053
$\varphi_2$	$B_d^0 \rightarrow \pi^+\pi^-$	$e^\pm$	60,000	0.60	1.0	0.7	0.47	0.062
$\varphi_2$	$B_d^0 \rightarrow \pi^+\pi^-$	$K^\pm$	460,000	0.40	1.0	0.7	0.47	0.033
$\varphi_3$	$B_s^0 \rightarrow \rho^0 K_S^0$	$e^\pm$	400	0.60	1.0	$\sim 10$	0.64	0.55
$\varphi_3$	$B_s^0 \rightarrow \rho^0 K_S^0$	$K^\pm$	3500	0.40	1.0	$\sim 10$	0.64	0.28
$\varphi_3$	$B_s^0 \rightarrow K^+K^-$	$e^\pm$	1,560	0.60	$\sim 0.1$	$\sim 10$	0.64	0.21
$\varphi_3$	$B_s^0 \rightarrow K^+K^-$	$K^\pm$	13,800	0.40	$\sim 0.1$	$\sim 10$	0.64	0.10
$\varphi_4$	$B_s^0 \rightarrow J/\psi\phi$	$K^\pm$	160,000	0.40	$\sim 0.1$	$\sim 10$	0.64	0.031

Table 1 includes a new feature since the writing of the BCD EOI, the Kaon tag, which is described in detail in section 4.1 below. Basically, the Kaon tag observes the sign of the

Kaon from the cascade decay chain  $b \rightarrow c \rightarrow s$  of the other  $B$  meson in the event. This tag can be confidently applied to the decay  $B_d^0 \rightarrow J/\psi K_S^0$  because the trigger for this will be the lepton pair from  $J/\psi$  decay. For other decay modes the Kaon tag could be applied only if a trigger such as on a secondary vertex can be developed, which is still somewhat speculative.

We have added a new line to Table 1 that includes an analysis of the decay  $B_s \rightarrow J/\psi \phi$ , which should have zero asymmetry (see p. 23 of the BCD EOI). We parametrize a possible nonzero asymmetry by  $\sin 2\varphi_4$ , and could set a good limit of 0.03 on this in one year.

The last column of Table 1 is calculated according to

$$\sin 2\varphi_{\min,3\sigma} = \frac{3(1+b)}{D(1-2p)\sqrt{N(1+b)+9}},$$

as discussed on pp. 27-29 of the BCD EOI.

We compare this sensitivity with that projected for an asymmetric  $e^+e^-$  collider following SLAC-353,<sup>[1]</sup> p. 25. This expresses the integrated luminosity needed to reach accuracy  $\delta(\sin 2\varphi)$  for one of the angles of the unitarity triangle as

$$\int \mathcal{L} dt = \left( 2\sigma(e^+e^- \rightarrow b\bar{b}) f_0 B \epsilon_r \epsilon_t [(1-2p)D\delta(\sin 2\varphi)]^2 \right)^{-1},$$

where

- $\sigma(e^+e^- \rightarrow b\bar{b}) = 1.2 \text{ nb}$  at the  $\Upsilon(4S)$ ,
- $f_0 = 0.5$  = fraction of  $B^0$ 's in  $b$ -quark fragmentation,
- $B$  = product of branching ratios to the desired final state  $f$ ,  
 $= 4.2 \times 10^{-5}$  for  $J/\psi K_S^0$ ,  
 $= 2 \times 10^{-5}$  for  $\pi^+\pi^-$ ,
- $\epsilon_r$  = reconstruction efficiency of  $f$ ,  
 $= 0.61$  for  $J/\psi K_S^0$ ,  
 $= 0.8$  for  $\pi^+\pi^-$ ,
- $\epsilon_t = 0.48$  = tagging efficiency,
- $p = 0.08$  = fraction of incorrect tags,
- $D = 0.61$  = tagging dilution factor.

The corresponding sensitivities to  $\sin 2\varphi_1$  and  $\sin 2\varphi_2$  at 3- $\sigma$  statistical significance are shown in Tables 2 and 3 for various amounts of running time, and at various luminosities.

We understand that a luminosity of  $3 \times 10^{33}$  is the current optimism for an asymmetric  $e^+e^-$  collider. It also seems agreed that a similar level of optimism is that a double-ring symmetric collider at Cornell could operate at a luminosity of  $10^{34}$ , which provides nearly identical sensitivity to  $\sin 2\varphi_1$  and  $\sin 2\varphi_2$  as that quoted above for an asymmetric collider.

An  $e^+e^-$  collider has little or no chance of measuring  $\sin 2\varphi_3$ , which requires reconstruction of the decay  $B_s \rightarrow \rho^0 K_S^0$ . SLAC-353,<sup>[1]</sup> p. 90, notes that it would require 2.5 years of running on the  $\Upsilon(5S)$  to achieve the accuracy projected by the BCD in Table 1, supposing the branching fraction is 500 times larger than that assumed by the BCD. If the branching ratio is indeed  $10^{-8}$  as suggested by Bauer, Stech, and Wirbel<sup>[6]</sup> and used by us, then it will require 1250 years of running at an  $e^+e^-$  collider to equal one year of running of the BCD.<sup>[2]</sup>

Note that the BCD is relatively more sensitive to  $\sin \varphi_2$  than  $\sin 2\varphi_1$  compared to the performance of an  $e^+e^-$  collider. This is because the transverse-momentum cuts on leptons

Table 2: The sensitivity of an asymmetric  $e^+e^-$  collider to  $\sin 2\varphi_1$  at 3- $\sigma$  statistical significance via the decay  $B_d^0 \rightarrow J/\psi K_S^0$ . A ‘year’ consists of  $10^7$  sec. The BCD sensitivity is 0.05 in one year of running.

$\mathcal{L}$ $\text{cm}^{-2}\text{sec}^{-1}$	Running Time (Years)		
	1	3	10
$10^{33}$	0.48	0.28	0.15
$3 \times 10^{33}$	0.28	0.16	0.09
$10^{34}$	0.15	0.09	0.05

must be higher at a hadron collider than at an  $e^+e^-$  collider, which reduces the sensitivity of the BCD to  $\sin 2\varphi_1$  somewhat. Also, experiments at an  $e^+e^-$  collider claim to reconstruct the decay  $K_S^0 \rightarrow \pi^0\pi^0$ , while the BCD does not.

Table 3: The sensitivity of an asymmetric  $e^+e^-$  collider to  $\sin 2\varphi_2$  at 3- $\sigma$  statistical significance via the decay  $B_d^0 \rightarrow \pi^+\pi^-$ . The BCD sensitivity is 0.06 in one year of running.

$\mathcal{L}$ $\text{cm}^{-2}\text{sec}^{-1}$	Running Time (Years)		
	1	3	10
$10^{33}$	0.61	0.35	0.19
$3 \times 10^{33}$	0.35	0.20	0.11
$10^{34}$	0.19	0.11	0.06

In summary of the SSC- $e^+e^-$  comparison:

- Both the BCD and an asymmetric  $e^+e^-$  collider seek high-quality measurements of  $CP$  violation in the  $B$  system. Either approach leads to a cost in excess of \$200M.
- The BCD detector is acknowledged to be more adventurous than that for an  $e^+e^-$  collider; the risk of the latter is in the accelerator performance.
- $\sigma_{b\bar{b}}$  at the SSC is  $10^6$  times that at the  $\Upsilon(4S)$  at an  $e^+e^-$  collider.  $\sigma_{b\bar{b}}/\sigma_{\text{tot}}$  at the SSC is 1/40 of that at the  $\Upsilon(4S)$ .
- The BCD is 30 times more effective per year than an asymmetric  $e^+e^-$  collider in measuring  $\sin 2\varphi_1$  and  $\sin 2\varphi_2$ .
- An asymmetric  $e^+e^-$  collider needs a luminosity of  $10^{35} \text{ cm}^{-2}\text{sec}^{-1}$  to be equivalent to the BCD at the SSC in measuring  $\sin 2\varphi_1$  and  $\sin 2\varphi_2$ . It would need  $5 \times 10^{36} \text{ cm}^{-2}\text{sec}^{-1}$  to be equivalent to the BCD for measuring  $\sin 2\varphi_3$ .

- An asymmetric  $e^+e^-$  collider cannot measure  $\sin 2\varphi_3$  at all (for  $\mathcal{L} < 10^{35}$ ).
- Thus the BCD is at least 30 times more cost effective in doing  $B$  physics than an asymmetric  $e^+e^-$  collider.
- The BCD will make other types of measurements, such as that of  $B$  decays with branching ratios as low as  $10^{-10}$ , and of the gluon structure function at very low  $x$ . The BCD also presents the capability for complete reconstruction of exotic high-mass particles that decay to all-charged final states.

## 1.2 $B$ Physics with Hadron Accelerators

When comparing the options for  $B$  physics at hadron accelerators we note that any such experiment must extract the signal in a high-multiplicity, high-rate environment. Fixed target experiments will be associated with a lower multiplicity, but particles are distributed over fewer units of rapidity, so the track density at the detectors is essentially the same as in a collider experiment. Thus to a first approximation the various options can be supposed to run at the same interaction rate, and assigned a relative figure of merit based simply on the ratio of the  $B\bar{B}$  cross section to the total inelastic cross section.

Table 4:  $B\bar{B}$  production at hadron accelerators. In this comparison we suppose that the experiments all operate at  $10^7$  interactions/sec, and that corresponding luminosity  $\mathcal{L}$  can be achieved. We then consider  $\sigma_{b\bar{b}}/\sigma_{\text{tot}}$ , as the figure of merit of the various accelerator options.

Accelerator	$\sqrt{s}$ (TeV)	$\sigma_{b\bar{b}}$ ( $\mu\text{b}$ )	$\sigma_{\text{tot}}$ (mb)	$\sigma_{b\bar{b}}/\sigma_{\text{tot}}$	$\mathcal{L}_{\text{ave}}$ ( $\text{cm}^{-2}\text{sec}^{-1}$ )	$N_{b\bar{b}}/10^7 \text{ sec}$	Figure of Merit
TEV II ( $p\text{-W}$ )	0.04	0.003	6	$5 \times 10^{-5}$	$1.7 \times 10^{33}$	$1.7 \times 10^7$	1/2500
SSC ( $p\text{-Si}$ )	0.2	3	15	1/5000	$6.7 \times 10^{32}$	$2 \times 10^{10}$	1/25
RHIC ( $p\text{-p}$ )	0.5	10	40	1/4000	$2.5 \times 10^{32}$	$2.5 \times 10^{10}$	1/20
TEV I ( $p\text{-}\bar{p}$ )	1.8	40	40	1/1000	$2.5 \times 10^{32}$	$10^{11}$	1/5
LHC ( $p\text{-p}$ )	16	250	75	1/300	$1.3 \times 10^{32}$	$3.3 \times 10^{11}$	2/3
SSC ( $p\text{-p}$ )	40	500	100	1/200	$10^{32}$	$5 \times 10^{11}$	1

This is presented in Table 4, which is a minor variation of Table 1 on p. 3 of the BCD EOI. The QCD estimates of  $\sigma_{b\bar{b}}$  are taken from Berger<sup>[3]</sup> for  $\sqrt{s} < 2$  TeV, and from Hinchliffe and Shapiro<sup>[4]</sup> for higher energies. The one reported measurement is that  $\sigma_{b\bar{b}} = 10.2 \pm 3.3 \mu\text{b}$  at  $\sqrt{s} = 0.63$  TeV,<sup>[5]</sup> compared to the estimate of  $13 \mu\text{b}$  of the model used here. For experiments with nuclear targets we suppose that the effective inelastic cross section per nucleon,  $\sigma_{\text{tot}}$ , is  $A^{-0.28}$  times that for  $p\text{-p}$  collisions.



### 1.2.1 Comparison of the BCD and SFT (SSC-EOI0014)

- **Physics Capability**

1. The physics capability of a fully instrumented BCD at the SSC collider is about 25 times that of a fully instrumented SFT in an SSC fixed-target beamline (see Table 4). While the BCD could measure  $CP$ -violating asymmetries in  $B$  decay down to 0.05 in one year of running, this would require 25 years of running with the SFT.
2. The SFT EOI gives no discussion of their capability for measuring  $\sin 2\varphi_2$ ,  $\sin 2\varphi_3$ , or  $B_s$  mixing.
3. In the discussion on p. 47 of the SFT EOI we note three factors are subject to question in making comparisons of sensitivity to  $\sin 2\varphi_1$ ; these factors are discussed further in paragraphs below. First, the total  $B\bar{B}$  sample will be at the low end of the stated range, based on present measurements of  $\sigma_{b\bar{b}}$ . Second, their branching ratio for  $B \rightarrow J/\psi K_S^0$  is twice the value measured at CLEO. Third, the fraction of  $B^\pm$  whose sign can be unambiguously determined in their vertex detector will be more like 1/8 than 1/2 due to the high density of tracks from the primary and secondary interactions in their target. By this argument we judge the SFT useful sample of tagged, reconstructed  $B \rightarrow J/\psi K^0$  to be only about 400 per year, 1/8 that of the minimum value they quote.
4. Hence the SFT could resolve  $\sin 2\varphi_1$  to 0.32 at  $3\text{-}\sigma$  significance in one year, assuming perfect tagging of the  $B^\pm$  but assessing the penalty for dilution due to mixing of the  $B_d^0$ .
5. The BCD is also 25 times more sensitive than SFT to rare  $B$ -decay modes. When extracting gluon structure functions from the  $B$ -production cross section the minimum  $x$  is of order  $M_B/\sqrt{s}$ , so the BCD can probe values of  $x$  about 200 times smaller than the SFT.
6. The SFT has capability equivalent to a mini-BCD experiment at the TEV I collider operating at a luminosity of  $5 \times 10^{31} \text{ cm}^{-2}\text{sec}^{-1}$ , which can be provided by the Main Injector Upgrade.

- **$\sigma_{b\bar{b}}$  Used in the SFT EOI**

The SFT EOI lists  $\sigma_{b\bar{b}}$  at  $\sqrt{s} = 0.2 \text{ TeV}$  as being in the range 2.5-10  $\mu\text{b}$ . However, it is clear from present knowledge that the value is at the low end of this range. As noted earlier,  $\sigma_{b\bar{b}}$  has been reported by UA1<sup>[6]</sup> to be  $10.2 \pm 3.3 \mu\text{b}$  at  $\sqrt{s} = 0.63 \text{ TeV}$ . Then using the  $\sqrt{s}$  dependence as calculated by Berger,<sup>[3]</sup> the best estimate is  $\sigma_{b\bar{b}} = (3/13)(10.2 \pm 3.3) = 2.3 \pm 0.8 \mu\text{b}$ . We have used a value of 3  $\mu\text{b}$  in the comparison of Table 4.

- **Inadequacy of the SFT Vertex Detector**

We believe the SFT vertex detector as proposed is inadequate to operate at the very high track densities experienced just downstream of a primary interaction.

Half of the 22 or so charged particles produced in an interaction will lie within a cone of half angle  $1/\gamma = 0.01$ . Then at a distance  $z$  (cm) downstream of the primary vertex there will be  $11$  tracks in  $200z \mu\text{m}$ , so the average separation between tracks is  $18z \mu\text{m}$ . With a silicon strip detector of  $25\text{-}\mu\text{m}$  pitch there will be 100% strip occupancy near the beamline for  $z$  up to 2 cm, and 10% occupancy for  $z$  up to 20 cm. Optimistically, the silicon detector could be used for tracking once  $z > 10$  cm from the primary vertex. This seems to defeat the purpose of the instrumented target, with only 6 mm between silicon planes.

Even though individual tracks will not be resolvable in the first 15 or so silicon planes, an analog measure to the total ionization will be available in principle. A 'multiplicity jump' signal might be sufficient to locate the first silicon plane after the primary vertex, but attempts to use this signature to locate secondary vertices in charm-production experiments have not met with success.

Even if the  $B$ -decay vertex is more than 10 cm downstream of the primary vertex, a new confusion will arise from the decay products of the  $B$ . A decay with charged multiplicity of 4 will deposit ionization in a block of adjacent  $25\text{-}\mu\text{m}$  strips for a distance of up to about 3 cm from the secondary vertex. Not only does this invalidate the proposed simple method of locating the secondary vertex, the block of struck strips renders large regions of the silicon detector unable to detect large-angle tracks that cannot be analyzed in downstream detectors where the track density is lower.

Of course, the development of high-rate pixel detectors capable of  $5\text{-}\mu\text{m}$  position resolution could make the instrumented target viable. Otherwise the premise of the SFT vertex detector seems invalid.

The BCD collaboration, but not the SFT collaboration, is participating in the development of pixel devices, together with Hughes Aircraft, U.C. Berkeley, and SLAC. A beam test of a prototype pixel detector has recently been made in the M-Test beam at Fermilab as part of T-784, the BCD R&D program.

#### • Secondary Interactions in the SFT Target

An effect not considered in the SFT EOI is secondary interactions in their target. In a typical interaction there will be about 30 secondaries with average lab momenta above 300 GeV/c, for which the  $J/\psi$  production cross section is about 100 nb/nucleon. The cross section for production for  $J/\psi$  from  $B$  decay is about  $3 \times 2 \times 0.01 \mu\text{b} = 60$  nb/nucleon. Then since the secondaries see only half the target length on average, the rate of secondary  $J/\psi$  production will be about 25 times that from  $B$  decay. The secondary interactions, of course, have a topology similar to the decay  $B \rightarrow J/\psi X$  at a secondary vertex, and will be the major component of a  $J/\psi$  trigger.

The effect of secondary  $J/\psi$  production could be reduced by a  $P_t$  cut in the trigger, at some expense in efficiency for  $J/\psi$ 's from  $B$  decay.

Because of the much lower energy of the secondaries at the SSC collider (within the acceptance of the BCD), and the smaller amount of material traversed by secondary particles, the secondary interactions are not a problem for the BCD.

---

- **Cost Effectiveness**

The  $B$ -decay products are spread over pseudorapidities  $-6 < \eta < 6$  at the SSC collider and over  $2.5 < \eta < 7.5$  at the SSC fixed-target. The cost of instrumentation varies roughly linearly with the rapidity interval, and will be the same for both experiments (if an equivalent physics quality is desired.) Hence the cost of a fully instrumented BCD is about 2.5 times that of a fully instrumented SFT. In the SFT proposal only 3 units of  $\eta$  are to be instrumented, while we propose to instrument 9 units in the BCD; hence we estimate the cost of the BCD to be 3 times that of the SFT as proposed. (The SFT cost estimate does not include the 40% for EDIA and Contingency as is applied to the BCD.) In terms of physics capability per dollar, the BCD is about 8 times more cost effective than SFT.

## 1.3 $B$ Physics in Other Collider Experiments

### 1.3.1 SSC: BCD and SDC

SSC experiments designed for Higgs-sector physics will have some capability for detection of  $B$ 's with high transverse momentum. But a high- $P_t$  detector with a moderate-rate data-acquisition system requires a minimum- $P_t$  cut of (at least) 20 GeV/ $c$  for a lepton trigger.  $B$ -decay products have an average transverse momentum of less than 2 GeV/ $c$ , and hence the high- $P_t$  experiment would be sensitive to only about  $e^{-10} = 5 \times 10^{-5}$  of all  $B$  decays, and only  $2.5 \times 10^{-9}$  of  $B\bar{B}$  pairs as needed for studies of  $CP$  violation. Even with a luminosity advantage of 100 over the BCD, such experiments will not have any statistical impact on studies of the physics of the CKM matrix and  $CP$  violation via  $B$  decays. This conclusion was seconded by G. Trilling at the June presentation of the EOI's.

With considerable modification to emphasize lower- $P_t$  particles, SDC or  $L^*$  would have increased capability for  $B$  physics. The modified detectors would need to run at luminosities lower than  $10^{33} \text{ cm}^{-2}\text{sec}^{-1}$ . See the following subsection for a comparison of how difficult it is to enhance CDF's capability for  $B$  physics once it has been optimized for high-mass, high- $P_t$  physics.

Detectors without a magnetic field have extremely limited capability for  $B$  physics in which full reconstruction of one  $B$  is essential. (At Snowmass an upgrade of D0 was discussed in which a magnet would be added to permit it to do  $B$  physics.)

### 1.3.2 TEV I: Mini-BCD and CDF

In the BCD EOI we remarked that the technical challenges of  $B$  physics could be more confidently met if there is an opportunity for an interim physics program at Fermilab that incorporates some of the advanced technology needed for the BCD at the SSC. It is natural to consider whether CDF upgrades provide such an opportunity, or whether a new, dedicated  $B$  collider experiment would be more appropriate. Here we make a comparison of such options, based in part on discussion with the  $B$ -Physics Working Group at Snowmass '90.

We conclude that a mini-BCD would have about 50 times the sensitivity of CDF for tagged, reconstructed decays involving a  $J/\psi$ , and 1000 times the sensitivity for decays that involve Kaons. The first category would give a mini-BCD access to the only very largest

Table 5: Geometric acceptance for single  $B$  decays, estimated with an ISAJET simulation. The geometric (and  $P_t$ ) cuts are described in the text. ‘mBCD’ = mini-BCD, ‘CDF’ = Collider Detector at Fermilab. The subscripts 1, and 2 refer to maximum angles of 20°, and 40°, respectively, for the forward arms of the mini-BCD.

Decay Mode	All-Charged Daughters	Detector		
		mBCD <sub>1</sub>	mBCD <sub>2</sub>	CDF
$B^+ \rightarrow \bar{D}^0 \pi^+$	$K^+ \pi^- \pi^+$	0.116	0.214	0.185
$B^+ \rightarrow D_s^+ \bar{D}^0$	$K^+ K^- \pi^+ K^+ \pi^-$	0.066	0.123	0.105
$B^+ \rightarrow J/\psi K^+$	$e^+ e^- K^+$	0.095	0.188	0.011
$B_d^0 \rightarrow D^- \pi^+$	$K^+ \pi^- \pi^- \pi^+$	0.072	0.141	0.121
$B_d^0 \rightarrow J/\psi K_S^0$	$e^+ e^- \pi^+ \pi^-$	0.044	0.095	0.005
$B_d^0 \rightarrow \pi^+ \pi^-$	$\pi^+ \pi^-$	0.383	0.613	0.251
$B_s^0 \rightarrow D_s^- \pi^+$	$K^+ K^- \pi^- \pi^+$	0.098	0.181	0.150
$B_s^0 \rightarrow D_s^- \pi^+$	$K^+ K^- \pi^- \pi^+ \pi^- \pi^+$	0.034	0.060	0.055
$B_s^0 \rightarrow D_s^- \pi^+ \pi^+ \pi^-$	$K^+ K^- \pi^- \pi^+ \pi^- \pi^+ \pi^-$	0.012	0.020	0.020
$B_s^0 \rightarrow \bar{D}^0 K^{*0}$	$K^+ \pi^- K^+ \pi^-$	0.075	0.145	0.134
$B_s^0 \rightarrow \rho^0 K_S^0$	$\pi^+ \pi^- \pi^+ \pi^-$	0.110	0.199	0.096
Average		0.100	0.180	0.103

signals for  $CP$  violation, but the second category of events would permit a good study of  $B_s$  mixing.<sup>[7]</sup>

In the CDF upgrade we suppose they adopt the BCD vertex detector with its 3-d reconstruction capability, as needed for low- $P_t$  tracks. In principle, CDF might also adopt a BCD-style data-acquisition system, and even implement a secondary-vertex trigger. However, as these would not enhance CDF’s capability for top-quark physics there is considerable skepticism that such upgrades could occur.

At CDF, we suppose that tracking is available for charged particles with  $P_t > 0.3$  GeV/ $c$ , and  $|\eta| < 1.25$ . There is no Kaon identification, but single lepton identification is available for  $P_t > 2$  GeV/ $c$  (B. Wicklund, private communication), and for  $|\eta| < 1.1$ . Single-lepton triggering, however, can only be done for  $P_t > 7.5$  GeV/ $c$ . Lepton-pair triggering can be done when each lepton has  $P_t > 2.5$  GeV/ $c$ .

We do not address here a more dramatic modification of CDF in which the vertex-TPC’s are replaced by silicon tracking, which could provide high-quality tracking over a larger rapidity interval. A quick calculation suggests that such an option might improve the yield for tagged, reconstructed  $B \rightarrow J/\psi K_S^0$  by a factor of 40 compared to that in Table 9.

The mini-BCD considered here would have smaller-scale versions of all the major subsystems of the full BCD. It consists of a central dipole magnet surrounding a silicon vertex detector and straw-tube tracking system. One forward arm is instrumented with Kaon and electron identification between angles 2 and 20° ( $1.7 < \eta < 4$ ), or 2 and 40° ( $1 < \eta < 4$ ).

We suppose the electron identification can be made to operate down to a  $P_t$  of 1 GeV/c, the demonstration of which would be a major goal of the mini-BCD. Tracking and Kaon identification is done for  $P_t > 0.3$  GeV/c. The mini-BCD would be triggered by lepton-pairs, single leptons, and secondary vertices. The last trigger is very ambitious, but would yield the greatest sensitivity to  $B_s$  mixing (which could also be studied via the single-lepton trigger).

Table 6: Rate estimates for reconstructed  $B$  decays, assuming 100% trigger efficiency. B.R.( $B$ ) is the branching ratio for the two-body  $B$  decay, estimated according to Bauer *et al.*<sup>[6]</sup> B.R.(Tot) is the product of B.R.( $B$ ) and the secondary branching ratios. The efficiency used is the product of the geometric acceptance from Table 5 and a factor 0.33 for the efficiency of tracking and vertexing. However, for the decays at CDF involving a  $J/\psi$  we suppose the vertexing efficiency is 0.9 due to the larger transverse momentum of the tracks. The reconstructed-event samples are for an integrated luminosity of  $500 \text{ pb}^{-1}$ , collectable in 1 year of running at a luminosity of  $5 \times 10^{31} \text{ cm}^{-2}\text{sec}^{-1}$ .

Decay Mode	All-Charged Daughters	B.R.( $B$ )	B.R.(Tot)	Recon. mBCD <sub>2</sub>	Decays CDF
$B^+ \rightarrow \bar{D}^0 \pi^+$	$K^+ \pi^- \pi^+$	0.004	$1.6 \times 10^{-4}$	160,000	140,000
$B^+ \rightarrow D_s^+ \bar{D}^0$	$K^+ K^- \pi^+ K^+ \pi^-$	0.008	$4.8 \times 10^{-6}$	2,900	2,500
$B^+ \rightarrow J/\psi K^+$	$e^+ e^- K^+$	$6 \times 10^{-4}$	$4.2 \times 10^{-5}$	39,000	6,200
$B_d^0 \rightarrow D^- \pi^+$	$K^+ \pi^- \pi^- \pi^+$	0.006	$4.8 \times 10^{-4}$	340,000	290,000
$B_d^0 \rightarrow J/\psi K_S^0$	$e^+ e^- \pi^+ \pi^-$	$3 \times 10^{-4}$	$1.4 \times 10^{-5}$	6,600	1,000
$B_d^0 \rightarrow \pi^+ \pi^-$	$\pi^+ \pi^-$	$2 \times 10^{-5}$	$2 \times 10^{-5}$	61,000	25,000
$B_s^0 \rightarrow D_s^- \pi^+$	$K^+ K^- \pi^- \pi^+$	0.005	$1.5 \times 10^{-4}$	90,000	74,000
$B_s^0 \rightarrow D_s^- \pi^+$	$K^+ K^- \pi^- \pi^+ \pi^- \pi^+$	0.005	$2 \times 10^{-4}$	40,000	36,000
$B_s^0 \rightarrow D_s^- \pi^+ \pi^+ \pi^-$	$K^+ K^- \pi^- \pi^+ \pi^- \pi^+ \pi^+ \pi^-$	0.01	$4 \times 10^{-4}$	26,000	26,000
$B_s^0 \rightarrow \bar{D}^0 K^{*0}$	$K^+ \pi^- K^+ \pi^-$	0.005	$1.3 \times 10^{-4}$	62,000	57,000
$B_s^0 \rightarrow \rho^0 K_S^0$	$\pi^+ \pi^- \pi^+ \pi^-$	$10^{-6}$	$7 \times 10^{-7}$	460	220

Tables 5 and 6 compare the acceptance and potential number of reconstructed  $B$  decays, assuming 100% triggering efficiency. The integrated luminosity assumed for Table 6 is  $500 \text{ pb}^{-1}$ , which could be collected in one year of  $10^7 \text{ sec}$  at a luminosity of  $5 \times 10^{31} \text{ cm}^{-2}\text{sec}^{-1}$  with the Main Ring Upgrade. Only for modes that involve a  $J/\psi$  is the triggering assumption valid in practice (*i.e.*, the efficiency of triggering on a lepton pair is already included in the Tables). The acceptance for decays without leptons is rather similar in CDF and a 40° mini-BCD. Of course, CDF has no Kaon identification so it is not immediately clear that the events with Kaons can be reconstructed by CDF. For decays with leptons the mini-BCD is about 6 times better than CDF, assuming that the minimum- $P_t$  cut for leptons in mini-BCD is actually 1 GeV/c.

However, all decays except those involving a  $J/\psi$  require a trigger on the second  $B$  in the event (unless a secondary-vertex trigger can be implemented.) We consider two possibilities;

Table 7: Acceptance for the tagging decay  $B_d^0 \rightarrow D^{*-}e^+\nu$ , estimated with an ISAJET simulation. For the electron tag we require the  $e^+$  and two of three hadrons. For the Kaon tag we require the Kaon and one other charged particle. Subscripts 1, 2, and 3 to CDF correspond to a minimum- $P_t$  cut of 5, 7.5, and 10 GeV/c for a single electron.

Decay Mode	All-Charged Daughters	Tag Type	Detector				
			mBCD <sub>1</sub>	mBCD <sub>2</sub>	CDF <sub>1</sub>	CDF <sub>2</sub>	CDF <sub>3</sub>
$B_d^0 \rightarrow D^{*-}e^+\nu$	$K^+\pi^-\pi^-e^+$	$e$	0.072	0.127	$6.4 \times 10^{-4}$	$3.3 \times 10^{-4}$	$2.9 \times 10^{-4}$
$B_d^0 \rightarrow D^{*-}e^+\nu$	$K^+\pi^-\pi^-e^+$	$K$	0.178	0.289	–	–	–

Table 8: Acceptance for tagged  $B$  decays, estimated with an ISAJET simulation. For the mini-BCD we use the 40° configuration and assume the Kaon tag is used; the acceptance includes a factor of 60% as the fraction of all decays of the second  $B$  that are useful for this tag. For CDF we use the lepton tag, and include a factor of 20% in the acceptance as the fraction of all decays of the second  $B$  that include an electron or muon. However, for the decays that include a  $J/\psi$  in CDF, a lepton-pair trigger can be used; then the tagging lepton from the second  $B$  need only be identified but not used in the trigger; in this case we have reduced the  $P_t$  threshold to 2.5 GeV/c. We use the decay  $B_d^0 \rightarrow D^{*-}e^+\nu$  to estimate the correlation in acceptance of the tagging and tagged  $B$ 's. The acceptances for the tagging decays only have been presented in Table 7 above.

Decay Mode	All-Charged Daughters	Detector	
		mBCD <sub>2</sub>	CDF <sub>2</sub>
$B^+ \rightarrow \bar{D}^0\pi^+$	$K^+\pi^-\pi^+$	0.070	$10 \times 10^{-5}$
$B^+ \rightarrow D_s^+\bar{D}^0$	$K^+K^-\pi^+K^+\pi^-$	0.041	$6.6 \times 10^{-5}$
$B^+ \rightarrow J/\psi K^+$	$e^+e^-K^+$	0.066	$20 \times 10^{-5}$
$B_d^0 \rightarrow D^-\pi^+$	$K^+\pi^-\pi^-\pi^+$	0.045	$13 \times 10^{-5}$
$B_d^0 \rightarrow J/\psi K_S^0$	$e^+e^-\pi^+\pi^-$	0.031	$10 \times 10^{-5}$
$B_d^0 \rightarrow \pi^+\pi^-$	$\pi^+\pi^-$	0.110	$10 \times 10^{-5}$
$B_s^0 \rightarrow D_s^-\pi^+$	$K^+K^-\pi^-\pi^+$	0.060	$3.3 \times 10^{-5}$
$B_s^0 \rightarrow D_s^-\pi^+$	$K^+K^-\pi^-\pi^+\pi^-\pi^+$	0.019	$6.6 \times 10^{-5}$
$B_s^0 \rightarrow D_s^-\pi^+\pi^+\pi^-$	$K^+K^-\pi^-\pi^+\pi^-\pi^+\pi^+\pi^-$	0.006	$< 10^{-5}$
$B_s^0 \rightarrow \bar{D}^0 K^{*0}$	$K^+\pi^-K^+\pi^-$	0.045	$1.0 \times 10^{-5}$
$B_s^0 \rightarrow \rho^0 K_S^0$	$\pi^+\pi^-\pi^+\pi^-$	0.037	$3.3 \times 10^{-5}$
Average		0.048	$7 \times 10^{-5}$

Table 9: Rate estimates for tagged and reconstructed  $B$  decays. B.R.( $B$ ) is the branching ratio for the two-body  $B$  decay, estimated according to Bauer *et al.*<sup>[6]</sup> B.R.(Tot) is the product of B.R.( $B$ ) and the secondary branching ratios. The efficiency used is the product of the geometric acceptance from Table 8 and a factor  $\epsilon$  for the efficiency of tracking and vertexing. For the mini-BCD we use the Kaon tag and take  $\epsilon = (0.33)^2 = 0.11$ , for CDF we use the lepton trigger and suppose that  $\epsilon = (0.33)(0.6) = 0.2$  for decays not involving a  $J/\psi$ , and  $\epsilon = (0.9)(0.6) = 0.54$  for those decays that do. The reconstructed-event samples are for an integrated luminosity of  $500 \text{ pb}^{-1}$ , collectable in 1 year of running at a luminosity of  $5 \times 10^{31} \text{ cm}^{-2}\text{sec}^{-1}$ .

Decay Mode	All-Charged Daughters	B.R.( $B$ )	B.R.(Tot)	Recon. Decays mBCD <sub>2</sub>	CDF
$B^+ \rightarrow \bar{D}^0 \pi^+$	$K^+ \pi^- \pi^+$	0.004	$1.6 \times 10^{-4}$	18,000	48
$B^+ \rightarrow D_s^+ \bar{D}^0$	$K^+ K^- \pi^+ K^+ \pi^-$	0.008	$4.8 \times 10^{-6}$	320	1
$B^+ \rightarrow J/\psi K^+$	$e^+ e^- K^+$	$6 \times 10^{-4}$	$4.2 \times 10^{-6}$	4,600	68
$B_d^0 \rightarrow D^- \pi^+$	$K^+ \pi^- \pi^- \pi^+$	0.006	$4.8 \times 10^{-4}$	36,000	187
$B_d^0 \rightarrow J/\psi K_S^0$	$e^+ e^- \pi^+ \pi^-$	$3 \times 10^{-4}$	$1.4 \times 10^{-5}$	720	12
$B_d^0 \rightarrow \pi^+ \pi^-$	$\pi^+ \pi^-$	$2 \times 10^{-5}$	$2 \times 10^{-5}$	3,600	6
$B_s^0 \rightarrow D_s^- \pi^+$	$K^+ K^- \pi^- \pi^+$	0.005	$1.5 \times 10^{-4}$	10,000	10
$B_s^0 \rightarrow D_s^- \pi^+$	$K^+ K^- \pi^- \pi^+ \pi^- \pi^+$	0.005	$2 \times 10^{-4}$	4,200	26
$B_s^0 \rightarrow D_s^- \pi^+ \pi^+ \pi^-$	$K^+ K^- \pi^- \pi^+ \pi^- \pi^+ \pi^+ \pi^-$	0.01	$4 \times 10^{-4}$	2,600	4
$B_s^0 \rightarrow \bar{D}^0 K^{*0}$	$K^+ \pi^- K^+ \pi^-$	0.005	$1.3 \times 10^{-4}$	6,400	3
$B_s^0 \rightarrow \rho^0 K_S^0$	$\pi^+ \pi^- \pi^+ \pi^-$	$10^{-6}$	$7 \times 10^{-7}$	28	0

a trigger on a single lepton, and a secondary-vertex trigger plus Kaon identification (possibly offline). The latter trigger cannot be implemented at CDF as presently configured because of the high-data rate implied by a secondary vertex trigger, and because of the lack of Kaon identification.

Table 7 shows our estimate of the geometric acceptance for the two types of triggers, which also have the merit of tagging the particle/antiparticle character of the second  $B$ . The lepton trigger applies to only 20% of all decays of the second  $B$  (if both electron and muon detectors are present), while 60% of the decays could be used for the Kaon trigger, as discussed in section 4.1 The secondary vertex trigger/Kaon tag at the mini-BCD would be about 1000 times more effective than the lepton trigger/tag at CDF.

Table 8 gives the combined acceptance for the decay of the first  $B$  and a tag via the second  $B$ . Table 9 the number of tagged, reconstructed events collectable in a run of  $500 \text{ pb}^{-1}$ .

The mini-BCD, with its optimistic trigger and tagging scenarios, should significantly outperform CDF according to our present understanding. We expect and encourage all possible progress at CDF to improve their capability for  $B$  physics, which may yield results

better than those estimated here.

A  $CP$ -violation study will require  $\sim 1000$  tagged, reconstructed events in decays to  $CP$  eigenstates such as  $J/\psi K_S^0$ ,  $\pi^+\pi^-$ , or  $\rho^0 K_S^0$ . The mini-BCD already comes close to this threshold for  $CP$ -violation physics at TEV I, and a full BCD would certainly exceed it. A sample of 720 tagged, reconstructed  $B \rightarrow J/\psi K_S^0$  events would measure  $\sin 2\varphi_1$  to  $3\text{-}\sigma$  accuracy if it is greater than  $2/3$  (which is within the presently allowed region). Note that a two-arm mini-BCD would have the same capability for measuring  $\sin 2\varphi_1$  as an asymmetric  $e^+e^-$  collider operating at a luminosity of  $10^{33} \text{ cm}^{-2}\text{sec}^{-1}$ , according to Table 2.

In the BCD EOI we estimated that a study of  $B_s$  mixing will require about 1500 tagged, reconstructed decays of  $B_s$  meson to self-tagging final states. This number assumed the use of a lepton tag. Supposing the Kaon tag (and secondary vertex trigger) can be implemented, the number of required tagged, reconstructed decays increases to about 4000. The large number is needed because of mistagging of the second  $B$ . However, it is quite appropriate to sum over all possible  $B_s$  decays, as they all have the same mixing parameter. Table 9 indicates that in the mini-BCD with  $40^\circ$  coverage some 23,000 tagged, reconstructed  $B_s$  decays can be collected in four relevant channels. Other channels will contribute at least an equal number of reconstructed events, and we judge that  $B_s$  mixing is within reach.

Note that the mini-BCD with  $20^\circ$  coverage would have  $1/4$  the acceptance for tagged, reconstructed decays, and would still be sufficient for a  $B_s$ -mixing study, albeit with little safety margin.

## 1.4 Non- $B$ Physics at the BCD

The BCD is designed to make precision measurements of a well-defined physics topic –  $CP$  violation in the  $B$ -meson system. The bulk of the papers published by the BCD collaboration will be on measurements of various quantities, in contrast to those of the Higgs-sector experiments, which will be about limits on unobserved particles.

As the BCD is designed to measure  $B$ 's, it can do non- $B$  physics that happens to involve  $B$  mesons. Examples are the extraction of the gluon structure function from the  $B$ -production cross section, and study of the decays  $t \rightarrow Wb$  and  $H \rightarrow b\bar{b}$ . The BCD will do an excellent job on the gluon structure function, but is not optimized for  $t$  and  $H$  studies.

The BCD has the ability to analyze high-momentum charged particles only in the forward direction, so if these particles arise from the decay of a heavy object the acceptance is limited. However, only the BCD among the SSC detectors will have hadron identification, which may permit it to detect exotic decays that are prominent at the SSC but which require Kaon identification (whether or not a  $B$  is involved).

The BCD will amass a very large sample of reconstructed charm decays as a background to  $B$  physics. The vertex detector and particle identification of the BCD are excellent tools for charm-decay analysis. As production of charmed mesons at the SSC is about 10 times that of  $B$  mesons, rather rare charm decays can be studied.

We have not made quantitative studies of the capability of the BCD for non- $B$  physics.



## 2 Doing $B$ Physics at a Hadron Collider

2. The committee acknowledges that the  $B$  production rate in the collider is very large. It is not convinced of the degree to which it can be exploited in the SSC environment.

- Please elaborate on the figure of 33% efficiency used for track finding and vertex association. What is the effect of additional minimum bias events within the sensitive time of the detector?
- Please estimate the efficiencies and mis-identification probabilities in the RICH, TOF, and lepton taggers.

From the tone of the question we presume the Committee is rightfully skeptical that any of the proposed major SSC experiments could be accomplished with existing technology. Because the BCD operates at a lower luminosity than the Higgs-sector experiments the detector occupancy is lower and pattern recognition is simpler. On the other hand, the BCD must have a much higher-rate data-acquisition system to accommodate the very large  $B$  production cross section, and the detector has particle identification systems that the other experiments do not.

We feel that an experiment for the year 2000 should not be limited to the technology of the 1980's, and so we have begun a vigorous R&D program towards demonstrating the improved detector performance needed for the SSC. A key aspect of the R&D is to bring the highly developed VLSI circuit technology into extensive use in high-energy physics. This will permit realistic operation of detectors with much larger channel count than at present. For example, the multiplicity at the SSC is about 2.5 times that at LEP, but the BCD will have 20 times more detector elements than any  $e^+e^-$  experiment.

### 2.1 $B$ -Meson Signals at CDF

As shown on p. 1 of the BCD EOI, CDF now has the largest sample of reconstructed  $B \rightarrow J/\psi K^\pm$  decays of any experiment. Since the PAC presentations additional signals of  $B \rightarrow J/\psi X$  have been demonstrated, for a total of about 50 reconstructed events; these are expected to be presented at the Singapore Conference. Note that the CDF results were obtained with no vertex detector, and no Kaon identification. Thus far only the muon-pair events have been analyzed; The sample size should increase as the electron-pair data are processed.

The  $B$ -physics Working Group from CDF at Snowmass 1990 estimates that the sample of reconstructed  $B$  decays will be 50 times larger after the 1991-92 run at Fermilab. This improvement comes from a factor of 5 increase in integrated luminosity, a factor of 2 from lower- $P_t$  lepton-pair triggers, a factor of 2 from increased muon coverage, and a factor of 2.5 from installation of the vertex detector. D. Cassell (private communication, 7/2/90) has estimated that by the end of 1992 the CLEO sample of reconstructed  $B \rightarrow J/\psi X$  decays will be 12 times larger than the present count of 11 events.

It is clear that in the  $J/\psi X$  channel, experiments at hadron colliders have already superseded those at  $e^+e^-$  colliders. Because CDF has no Kaon identification (and likely never will), and its single-lepton trigger is at 10 GeV/ $c$ , its capability for nonleptonic decays is

restricted compared to that of an  $e^+e^-$  collider. This is due to the optimization of CDF for top-quark physics rather than an intrinsic limitation of hadron colliders.

## 2.2 Vertexing Efficiency

Figure 1 shows the simulated efficiency for reconstruction of a secondary vertex for two- and four-body  $B$  decays as a function of the minimum-transverse momentum cut applied on individual tracks. With a cut of 0.3 GeV/c, the simulation suggests an efficiency of 0.33, as was assumed in the BCD EOI.

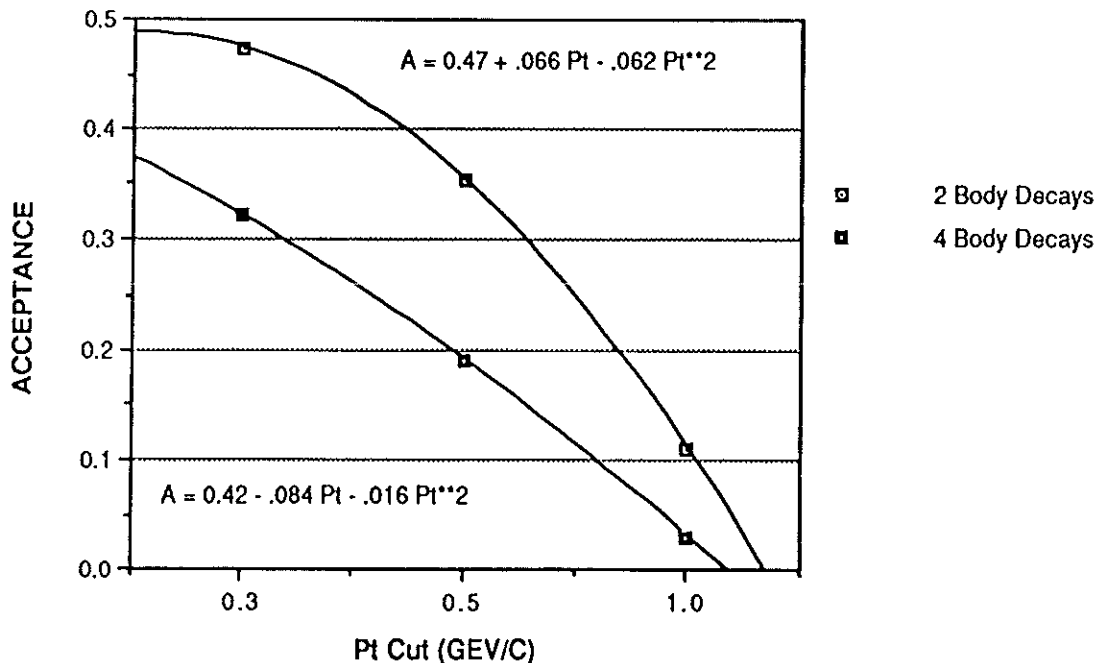


Figure 1: Monte Carlo simulation of the efficiency of reconstruction of a secondary vertex for two- and four-body  $B$  decays, as a function of the minimum  $P_t$  required for each track. The results also include the geometric acceptance of the detector for the tracks, but do not include an efficiency for track pattern recognition.

As details of this simulation have not been provided elsewhere we append them here.

Note that the vertex efficiency simulation does not address the important question of the efficiency of track pattern recognition in the presence of detector inefficiencies and overlapping hits. However, as the ability of the BCD vertex detector to locate the vertices is of critical significance, we consider it relevant to explore the vertex efficiency even assuming perfect track pattern recognition. Tracking errors due to multiple scattering and finite detector resolution are simulated, and lead to inefficiencies in vertex finding, especially for  $B$  decays after very short flight paths.

A preliminary issue is the spatial resolution of the silicon strip detectors for tracks with large angles of incidence on the silicon wafers. Tracks with, for example,  $45^\circ$  incidence

create only 5600 electron-hole pairs in a strip 50  $\mu\text{m}$  wide. The readout electronics must have very low noise to resolve this small signal. Figure 2 shows the simulated position resolution *vs.* angle of incidence in a silicon strip detector with 25- $\mu\text{m}$  strips every second of which is read out via amplifiers with 600-electrons noise equivalent. This noise, as well as Landau fluctuations in the ionization, are simulated. The amplified signals are digitized in a (simulated) 8-bit ADC to permit centroid finding for the cluster of hits due to a 'dip' track. The results indicate that rather good position resolution can be expected for tracks with angles of incidence up to 70°.

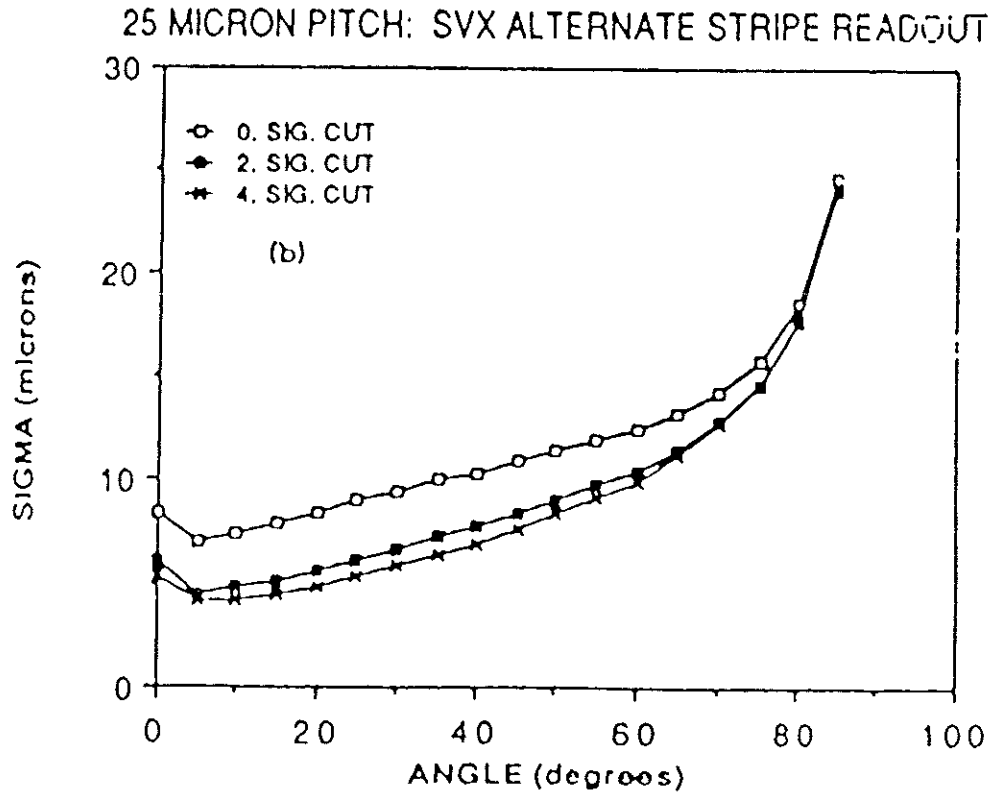


Figure 2: Simulation of the spatial resolution obtained in a silicon strip detector with 25- $\mu\text{m}$  strip width, with every second strip readout and digitized, as a function of the angle of incidence of the track on the silicon wafer. Good resolution holds for angles up to 70° if the individual strip signals remain above the noise level and can be included in a centroid calculation.

An ISAJET/GEANT simulation of the BCD vertex detector was used to generate lists of hits on tracks from  $p$ - $p$  collisions that can be specified to have produced a  $B$ - $\bar{B}$  pair. Tracks are fit to these hits, and the track error matrix estimated based on models of the multiple scattering and detector resolution. The tracks are then fit to a common vertex using a standard routine from the CERN library. The track that has the largest  $\chi^2 > 4$  to the vertex hypothesis is removed from the fit, and the fit iterated. Tracks are removed until all remaining tracks fit to the vertex with  $\chi^2 < 4$ . The set of tracks not fitting to the first vertex are then searched for secondary vertices by the same procedure, until all

tracks belong to some vertex, or fail to fit to any vertex. Subsidiary algorithms with slightly different cuts reconsider those tracks not fitting to any vertex in an attempt to place them on some vertex. The vertex with the largest number of tracks is declared to be the primary vertex. At present, no constraint involving knowledge of the primary beamsize has been used, although this will be powerful in later practice. The vertex reconstruction algorithm is quite computer intensive.

The Monte Carlo simulation, of course, has available the generated vertex and track parameters for comparison with the reconstructed quantities. Figure 3 shows the distribution of distance in space between the true and reconstructed vertices for the primary interaction, and for a sample of  $B \rightarrow \pi^+\pi^-$  decays. The most probable error is  $25 \mu\text{m}$ , with a long tail. The tail is due to events in which very few central tracks are available; forward tracks give lower precision in locating the vertex. Figure 4 shows the spectrum of distances between reconstructed primary and secondary vertices. The mean is  $2.2 \text{ mm}$ , but secondary vertices as close as  $100 \mu\text{m}$  to the primary can be reconstructed with fair efficiency.

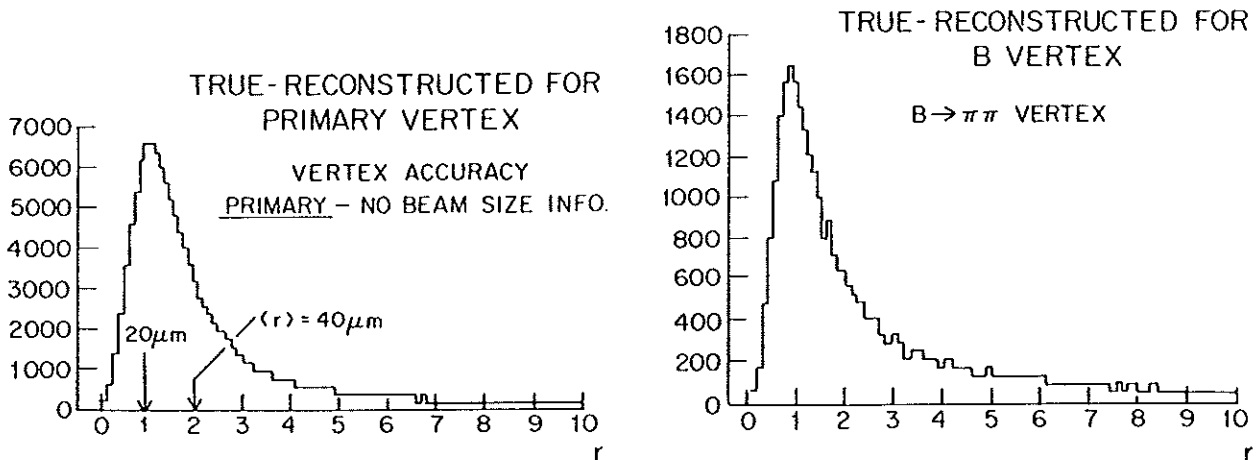


Figure 3: Simulated spectrum of distances between the true and reconstructed vertex positions for primary and secondary vertices.

In the attempt to isolate true secondary vertices we apply further cuts. As anticipated in Fig. 1, one of these is a minimum- $P_t$  requirement for each track. Figure 5 illustrates that pions from the two-body decay  $B \rightarrow \pi^+\pi^-$  have considerably larger  $P_t$  than the background of non- $B$  decay products. Also, tracks with low transverse momentum suffer greater multiple scattering in the detector and are more likely to yield a bad fit to the primary vertex, possibly faking a secondary vertex. However, for higher multiplicity  $B$  decays the acceptance drops rapidly on increasing the minimum- $P_t$  cut, and a cut at  $0.3 \text{ GeV}/c$  seems indicated. In a background-prone mode such as  $B \rightarrow \pi^+\pi^-$  a higher cut may be desirable.

Another cut to distinguish true secondary vertices is the requirement that the total-momentum vector of the secondary vertex point back to the primary vertex. We implemented

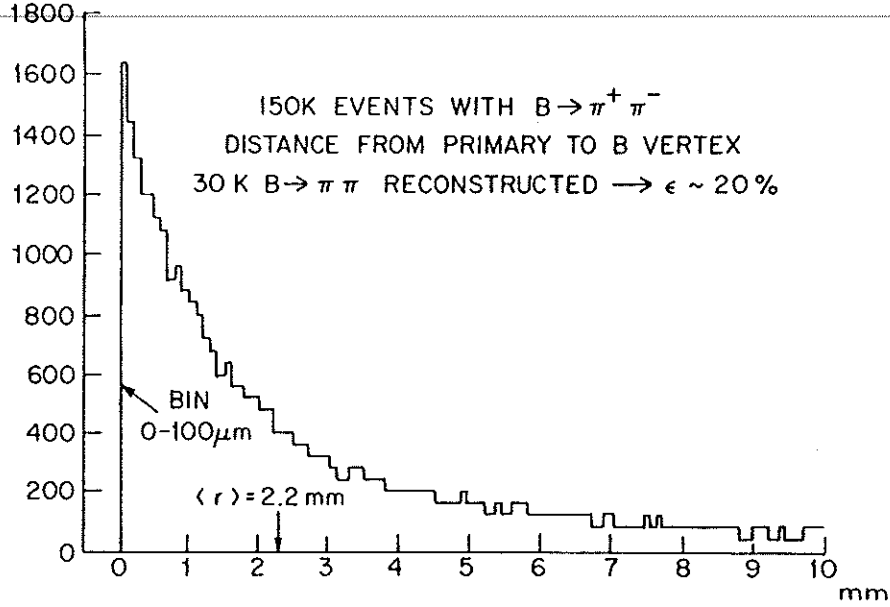


Figure 4: Simulated spectrum of distances between reconstructed primary and  $B$ -decay vertices.

this via a cut on the closest distance of approach between the primary vertex and the momentum vector of the secondary vertex, as illustrated in Fig. 6.

The final cut on secondary-vertex quality examines the ratio  $S/\delta S$  where  $S$  is the distance between the primary and secondary vertex, and  $\delta S$  is the error on  $S$ , evaluated using the output errors matrices from the vertex fits. Figure 7 illustrates how  $S/\delta S$  is peaked at small values for ‘fake’ secondary vertices, while having a mean value of 18 for reconstructed vertices from  $B \rightarrow \pi\pi$ . Here we generated 150k events containing  $b\bar{b}$  jets and asked the computer to find all secondary vertices. Most of these are due to tracks with fitting errors large enough that they do not properly reconstruct to the primary vertex. However, a secondary vertex made from two such tracks is typically of poor quality and does not survive the  $S/\delta S$  cut.

The vertex study provides estimates of the efficiency for reconstruction of true secondary vertices as shown in Fig. 1, but also allows us to estimate the background to the  $B$ -decay signal due to misreconstructions. After generating events containing  $B$  mesons, and charmed mesons, as well as minimum-bias events, we find that the greatest problem arises from events that contain  $B$ ’s, assuming charm production is no more than 10 times that of  $B$  production. The most probable way of obtaining a secondary vertex whose mass fits to that of the  $B$  is to have one good track from a  $B$  decay mismatched with a track from the primary vertex that gave a better fit to a secondary vertex with the  $B$  track. This is illustrated in Figs. 8 and 9 which show the mass spectrum for ‘fake’ two-track secondary vertices found in events containing  $B$  mesons and charmed mesons, respectively. Note that these ‘fake’ vertices include some true secondary vertices due to  $K$  and  $D$  mesons. The shoulder between 1 and 2  $\text{GeV}/c^2$  is due to two-track vertices made from three-or-more-body decays of  $D$  mesons, while that between 2 and 5  $\text{GeV}/c^2$  is due to partially reconstructed  $B$  decays. The latter is, of course, not seen in Fig. 9 whose event sample contained no  $B$ ’s.

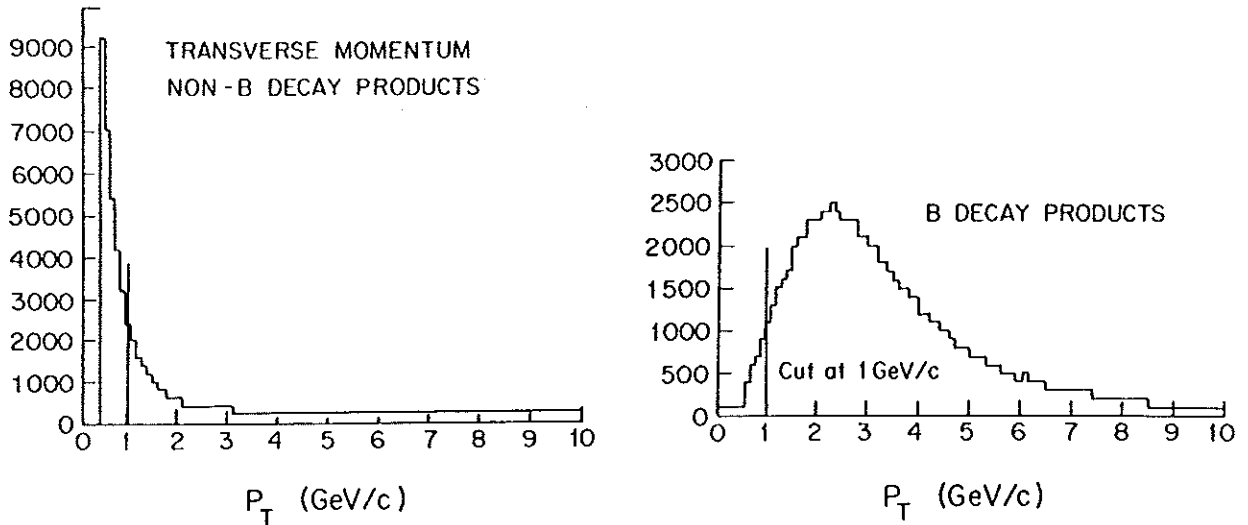


Figure 5: Simulated  $P_T$  spectra for  $B$ - and non- $B$ -decay products. The  $B$  decay illustrated here is  $B \rightarrow \pi\pi$ .

From this study we estimate that the signal to noise will be about 1:1 for the decay  $B \rightarrow \pi\pi$  whose branching ratio is expected to be  $2 \times 10^{-5}$ . This will be one of the most background-prone  $B$  decays because it is only two-body, so a single bad primary track can combine with a  $B$ -decay track to yield the fake vertex. There is no suppression available via particle identification, as only pions are involved, and there is no cascade decay chain that would permit additional mass constraints to improve the signal.

### 2.3 Tracking Efficiency

Studies of the tracking efficiency at the BCD are underway both for the silicon vertex detector and for the straw-tube tracking system. Thus far the results of the studies have not been integrated with the vertexing study to indicate the loss of signal to noise due to tracking errors.

A sense of the tracking difficulties in the vertex detector was given in Fig. 14 on p. 40 of the BCD EOI. This indicates the probability of a false hit being associated with a track in the vertex detector due to other tracks or to noise fluctuation in the readout amplifiers. The BCD design will implement strip lengths such that this 'confusion' probability is 1% per hit. Then since an average track has 5 hits in the vertex detector there would be a 5% probability that each track has one false hit in the pattern roads. Bad hits can be rejected with some probability by the iterative  $\chi^2$  fitting algorithm. As noted above, the ultimate effect of the remaining bad hits on the physics has not been assessed yet. The probability that a track in the silicon vertex detector has enough hits that a track can be fit is over 99%.

Preliminary results from a simulation of the straw-tube tracking were reported in section 4.2.4 of the BCD EOI. The track-finding algorithm successfully associated 91% of the

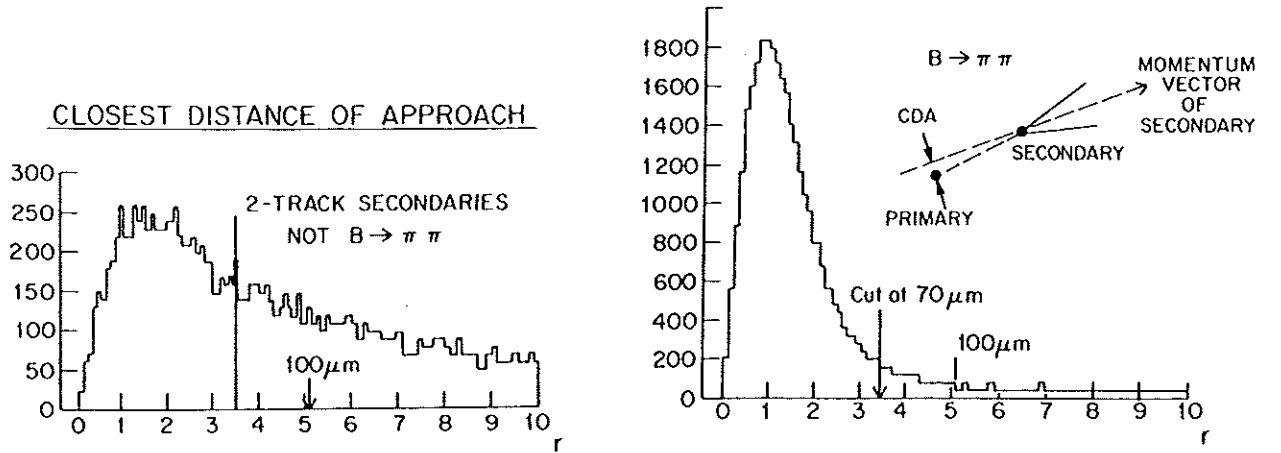


Figure 6: Simulated spectra of closest distance of approach between the primary vertex and the total-momentum vector of a secondary vertex, for 2-track secondary vertices.

'minivectors' with the proper track. Each track has an average of 8 minivectors, so on average one is missing per track at this early stage of simulation. If we require at least 5 found minivectors to define a track, the tracking efficiency will be about 98%.

## 2.4 Effect of Multiple Interactions

The design luminosity of the BCD is  $10^{32} \text{ cm}^{-2}\text{sec}^{-1}$ , at which there would be one primary interaction every 6 bunch crossings. Thus one in six interaction would be associated with a second primary interaction in the same bunch crossing.

The multiple-interaction rate is small enough that BCD will have the option of simply rejecting events that appear to involve multiple primary interactions.

Nonetheless the BCD will endeavor to utilize the multiple interactions, but our capability for this is not well studied at present. An immediate concern is the effect of the larger number of struck detector elements on pattern recognition. The efficiency of track reconstruction and particle identification will undoubtedly be less in multiple-interaction events.

The one study that we have performed is on vertex finding in multiple events, supposing that the track finding efficiency is 100%. Then we found, as was to be expected, that if the primary vertices are separated by more than about  $200 \mu\text{m}$ , both vertices are found with a quality similar to that in single-interaction events. As the primary interaction vertices will be distributed over a length of more than 10 cm, the vertexing inefficiency due to multiple interactions will be less than 1%, in the limited sense of this study.

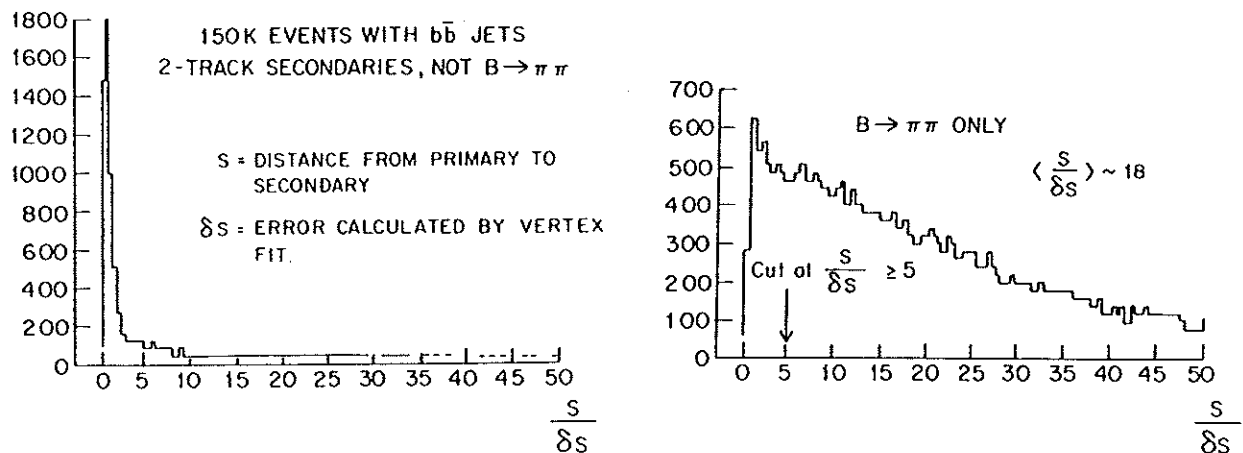


Figure 7: Simulated spectra of  $S/\delta S$ , where  $S$  is the distance between the primary and secondary vertices, for 'fake' and real two-track secondary vertices.

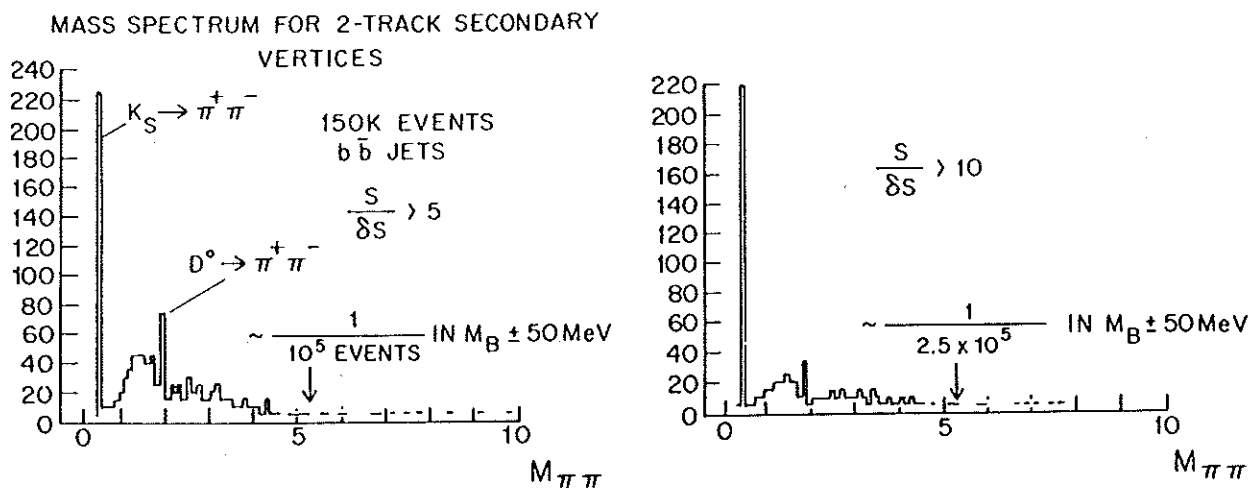


Figure 8: Simulated mass spectrum of 'fake' two-track secondary vertices found in event containing  $B$ 's, for two values of the  $S/\delta S$  cut. Many of the 'fake' secondary vertices are due to full or partial reconstructions of  $B$ ,  $D$ , and  $K$  decays.



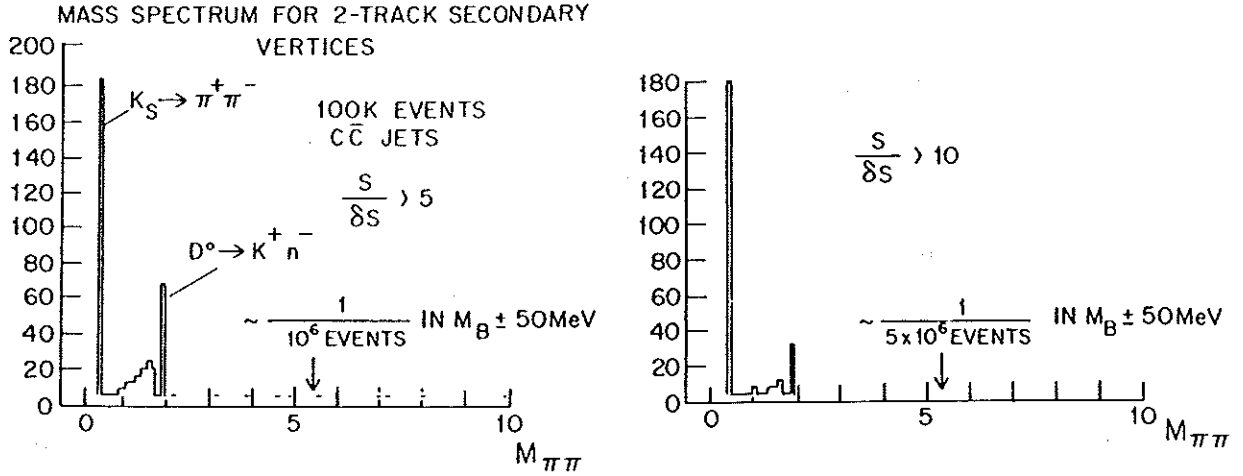


Figure 9: Simulated mass spectrum of 'fake' two-track secondary vertices found in event containing  $D$ 's, for two values of the  $S/\delta S$  cut.

## 2.5 Efficiency of Particle Identification

There is little direct experimental evidence at hadron colliders as to the efficiency of the particle identification techniques proposed for the BCD. No other major SSC experiment proposes to have hadron identification, and they incorporate electron identification only at transverse momenta much higher than are relevant for a  $B$ -physics experiment. We feel it is important that laboratory evidence be obtained to supplement Monte Carlo estimates, and have proposed R&D projects to this end as part of the BCD EOI.

The RICH counter system will be designed to yield 25 detected photoelectrons per high-momentum charged particle. With this, the efficiency for recognizing a ring would be essentially 100% in the absence of overlapping hits from other particles. The granularity of the 'smart pads' is chosen so that the average probability of multiple hits is about 1.5% per pad. Only about 1/2 of the pads along a ring generate photoelectrons from the particle of interest, so there will be about 1 extraneous hit per ring of pads per particle. Some fraction of the time this will cause the radius of the ring to be misestimated and the particle misidentified. We believe the misidentification probability will be less than 10%.

The granularity of the Time-of-Flight system has been chosen so that the probability of an extra hit from a charged particle is 1%. In addition, there will be hits from converted photons and neutrons, including those reflected from the electromagnetic calorimeter. We estimate the total probability of an extra hit to be 3%. For counters read out from one end only, as in the BCD design, an extra hit implies a 50% probability of a bad timing measurement, and hence about 1.5% misidentification probability.

Electron identification is accomplished through a combination of the TRD system and the electromagnetic calorimeter. As stated in the BCD EOI, the TRD design goals are 90% electron efficiency with 1% probability that a pion is called an electron. The overall electron-

identification goal is 80% electron efficiency, with  $10^{-5}$  probability of misidentification of a pion.

### 3 BCD at Very High Luminosity

3. *Will it be possible to use higher luminosity for specific (and simple) rare decay modes?*

The BCD operating at a luminosity of  $10^{32} \text{ cm}^{-2}\text{sec}^{-1}$  is already an excellent detector for rare  $B$  decays. For example, the branching fraction  $B \rightarrow \mu^+\mu^-$  may be as low as  $10^{-9}$ ,<sup>[8]</sup> so in excess of 100 events per year above background will be reconstructed.

The BCD has full coverage of the allowed region of  $\sin 2\varphi_1$  within the present experimental understanding of the Standard Model. Should the value of  $\sin 2\varphi_1$  prove to be smaller we could pursue it in higher-luminosity running via the decay  $B \rightarrow J/\psi K_S^0$  with a trigger on the lepton pair.

The BCD front-end electronics will be designed to operate with the SSC bunch-crossing period of 16 ns, consistent with a luminosity of  $10^{33} \text{ cm}^{-2}\text{sec}^{-1}$ . However, the vertex-detector front-end electronics, and the inner straw tubes are subject to radiation damage at this luminosity.

The radiation-damage limits to the silicon detectors and electronics are discussed in the BCD EOI on pp. 46-47. The radiation limit is  $\sim 5$  Mrads for *rad-hard* CMOS technologies, while the dose due to the charged-particle flux through the electronics 30 MRad/ $R^2$  per year at  $10^{33}$  luminosity. Then the minimum usable radius would be 5 cm instead of 1.5 cm as for  $10^{32}$  luminosity. For low-momentum tracks for which the vertex resolution is dominated by multiple Coulomb scattering, the vertex resolution would be degraded by a factor of 3 compared to running at  $10^{32}$  luminosity.

At  $10^{33}$  luminosity, the minimum usable radius of the straw-tube system would be at  $\sim 50$  cm instead of 15 cm, due to coating of the anode wires with insulating polymers from chamber gas cracked by high-radiation levels. In this case the pattern recognition capability would be degraded.

The radiation damage to the inner vertex and tracking detectors would likely be permanent. The high-luminosity option would be exercised with care!

In summary, we expect operation of the BCD is possible at a luminosity of  $10^{33}$  with degraded performance for tracking and vertexing.

### 4 Sensitivity to CKM Angle $\varphi_3$ Via $B_s$ Decays

4. *Please discuss in more detail the proposed measurement of the angle  $\varphi_3$  via the decay of the  $B_s$ . Estimate the detection efficiency, the dilution of the measurement due to impurities in the tag and  $CP$  sample, and the achievable statistical and systematic errors.*

The study of the interior angles of the unitarity triangle via the decays of neutral  $B$  mesons to  $CP$  eigenstates requires these decays to be tagged as to their particle/antiparticle character. This will be accomplished by a partial reconstruction of the companion  $B$  in the event. We first present a possible improvement in the tagging over that discussed in the BCD

EOI. Studies of the signal to noise for the decay  $B_s \rightarrow \rho^0 K_S^0$  are in progress, but results are not available at present.

## 4.1 Tagging with Kaons

In the BCD EOI we discussed a lepton tag and hinted at other possibilities. Here we examine the possibility of tagging on the sign of a charged Kaon from the decay of the second  $B$  in the event. Such a Kaon would not reconstruct to the primary event vertex. This tag might be combined with a secondary-vertex trigger if the latter can be devised. It certainly could be used with a dilepton trigger, which would be useful in enlarging our samples of tagged  $B \rightarrow J/\psi X$ .

Recall the problem with the lepton tag. Only 20% of the  $B$ 's decay to an electron or muon; the acceptance for these is only about 40% (due to the  $P_t$  cut), and the vertexing efficiency is estimated at 33%. Hence only 2.7% of all decays could be tagged this way. [In the EOI, the 2 chances for an interesting  $B$  decay per  $B\text{-}\bar{B}$  pair are included elsewhere in the bookkeeping.] Furthermore, all tagging will be subject to a  $p = 20\%$  mistagging probability due to mixing. The proper figure of merit is  $1 - 2p = 60\%$ , so the fraction of  $B$  decays effectively tagged by the lepton tag is only about 1.6%.

The Kaon tag would be based on the sign of the Kaon arising in the decay chain

$$b \rightarrow c \rightarrow s \rightarrow K^- \quad \text{or} \quad \bar{K}^0.$$

This chain occurs  $\sim 95\%$  of the time. [In Table 10 below, we suppose this chain occurs 100% of the time.] However, the  $b \rightarrow c$  transition includes the emission of a  $W^-$ , which can decay to a  $\bar{c}s$  combination about 33% of the time; then the  $\bar{c}$  decays to a  $\bar{s}$  essentially 100% of the time. The  $s(\bar{s})$  quark emerges as a  $K^-(K^+)$  50% of the time. The presence of a  $K^+$  could lead to a mistag. In the case of multiple Kaons, we just choose one at random to be the tagging Kaon, and suffer the consequences. Table 10 summarizes the probabilities of various qualities of tags occurring.

Table 10 ignores the small probability that an  $s\bar{s}$  pair is created from glue. This, and some of the 'Bad Tags' listed in the Table 10, could likely be suppressed by a momentum cut, not explored here. There is typically an extra Kaon in  $B_s$  decays, which would lead to bad tags. However,  $B_s$  decays are useless as tags because of their rapid oscillations; this dilution is already accounted for in the 20% mistagging probability due to mixing.

From Table 10 we see that  $45/72 = 62\%$  of all  $B$  decays could yield a Kaon tag, but that  $7/45 = 16\%$  of these would be a mistag. Actually, we must combine the mistags due to the wrong-sign Kaon with the mistags due to mixing. The total mistagging probability is  $(16\%)(80\%) + (84\%)(20\%) = 30\%$ . The tagging efficiency is then  $1 - 2p = 40\%$ . We estimate that the geometrical acceptance for the Kaon tag would be more like 70%, as we wouldn't need as strong a  $P_t$  cut as for the leptons. The vertexing efficiency is again about 33%. Hence the effective fraction of  $B$  events that could have a Kaon tag is  $(70\%)(33\%)(62\%)(40\%) = 6\%$ .

This is four times higher than the lepton tag. It is fairly likely that we could make this tag work for the  $B \rightarrow J/\psi X$  events, and so the useful tagged, reconstructed event sample in the EOI should be multiplied by up to 4. This would improve our sensitivity to  $\sin 2\varphi_1$

Table 10: Estimates of the efficiency of a tag on the particle/antiparticle character of a  $B$  meson based on the sign of Kaons in the  $B$  decay.

$b \rightarrow c \rightarrow s \rightarrow$	$b \rightarrow W^- \rightarrow$	Good Tag Prob.	Bad Tag Prob.	No Tag Prob.
$K^-$	other	1/3		
$K^-$	$K^+ \bar{K}^0$	1/48	1/48	
$K^-$	$K^+ K^-$	2/72	1/72	
$K^-$	$K^0 \bar{K}^0$	1/24		
$K^-$	$K^0 K^-$	1/24		
$\bar{K}^0$	other			1/3
$\bar{K}^0$	$K^+ \bar{K}^0$		1/24	
$\bar{K}^0$	$K^+ K^-$	1/48	1/48	
$\bar{K}^0$	$K^0 \bar{K}^0$			1/24
$\bar{K}^0$	$K^0 K^-$	1/24		
Total		38/72	7/72	27/72

by 2, bringing it down to 0.05, as summarized in Table 1 (but calculated in more detail by slightly different logic).

If a secondary-vertex trigger could be implemented, we might get this improvement in all tagged, reconstructed event samples. To stimulate further discussions, we include the effect of a successful implementation of the Kaon tag for all  $B$ -decay modes in Table 1.

An even more aggressive use of Kaon tagging of  $B_s$  mesons has been proposed by P. Schlein.<sup>[9]</sup> He argues that even if no secondary Kaon is available for tagging there may be one from the primary vertex from an associated production. In our estimate, only 25% of the  $B_s$  ( $\bar{b}s$ ) mesons would be accompanied by a  $\bar{B}_s$ ; 75% of the time the associated  $\bar{s}$  quark would be in a Kaon and 37.5% of the time the  $\bar{s}$  would be in a  $K^+$ . This  $K^+$  could be used for tagging. However, an SSC event with  $\sim 60$  charged tracks would typically have 6 charged Kaons, and so 3  $K^-$ . These would be distributed over  $\sim 12$  units of rapidity. The tagging  $K^+$  will be within  $\sim \pm 1$  unit of rapidity from the  $B_s$ , and there is  $\sim 50\%$  probability that there is a  $K^-$  in the same interval. Hence the mistagging probability is about 30%. If we adopt this technique along with the tag on Kaons from the other  $B$ , the Kaon tag would be available for 72% of all  $B_s$ , with an overall tagging efficiency of 40%. This is only a slight improvement over tagging only with Kaons from the second  $B$ .

These arguments reinforce the interest in exploring the trigger and tag in a mini-BCD experiment. Of course, we must have Kaon identification to implement the Kaon tag.

## 5 Alternative Detector Configurations and Staging

*5. It is unlikely that there will be enough money to meet all requests initially. How can this detector be staged? What costs can be deferred? What are the physics capabilities at each stage?*

### 5.1 Alternative Detector Configurations

The cost of instrumenting the BCD is roughly linear in the rapidity interval covered, while the acceptance for tagged, reconstructed  $B$  decays varies roughly with the square of the rapidity interval. Hence alternatives to the BCD with less coverage have considerably reduced cost effectiveness. To maximize the eventual  $B$  physics we only contemplate alternative configurations that could be upgraded to the full potential of the BCD.

The BCD is built of many different detector subsystems, so configurations with less than the full complement of detectors are readily contemplated. In Table 11 we list 14 detector subsystems which are then considered in various combinations in Tables 12 and 13. Of the  $2^{14}$  conceivable detectors ranging in cost from \$0 to \$235M, we present 25 configurations to illustrate some of the more interesting options.

In Table 12 we consider configurations that maintain a capability for both hadron and lepton identification at an early stage, and hence pursue a broad range of  $B$  physics topics with limited acceptance. In Table 13 we emphasize lepton identification only, which is sufficient for study of  $\sin 2\varphi_1$  and  $\sin 2\varphi_2$ , but is not optimal for  $B_s$  mixing and  $\sin 2\varphi_3$ . Relative figures of merit are assigned on a price/performance basis.

The physics capability of each option has been estimated from Table 7 on p. 12 of the BCD EOI, while the cost has been estimated from the cost table on p. 98 of the BCD EOI. As in the EOI, we do not consider the use of muon detection in the Central Region because of the low momentum of the  $B$ -decay muons there.

For configurations in which the muon detector is not implemented we suppose the effective acceptance is 1/2 as large (in the relevant detector region). For studies with an electron tag and a  $J/\psi$  in the other- $B$  final state the acceptance is only 1/4 as large, but if a secondary-vertex trigger is implemented there is no change in acceptance for modes with a  $J/\psi$ .

Recall that the BCD consists of three detector regions, Central, Intermediate, and Forward. Both the Intermediate and Forward Regions are composed of two arms on either side of the interaction point.

In Table 12, configurations A-F explore the merits of implementing only one detector region. Any one has rather low acceptance, but as noted in the EOI, the Intermediate Region is the most important.

Configurations G-J consider implementing two detector regions. It appears that Central + Intermediate is roughly equivalent to Intermediate + Forward, as was noted in the EOI.

Configurations K and L consider implementing only one arm of the detector, but with all three regions instrumented. About 50% of maximal acceptance can be achieved, but the detector cost is 74% of maximum.

Configurations M and N consider the Central detector plus both Intermediate arms. The quality is very similar to configurations K and L.

Table 11: The 14 detector subsystems considered in various combinations in Table 12.

Detector Acronym	Detector Type	Detector Region
$\mu$ F1	Muon identification	Forward Arm 1
eF1	Electron identification	Forward Arm 1
hF1	Hadron identification	Forward Arm 1
$\mu$ I1	Muon identification	Intermediate Arm 1
eI1	Electron identification	Intermediate Arm 1
hI1	Hadron identification	Intermediate Arm 1
eC	Electron identification	Central
hC	Hadron identification	Central
$\mu$ I2	Muon identification	Intermediate Arm 2
eI2	Electron identification	Intermediate Arm 2
hI2	Hadron identification	Intermediate Arm 2
$\mu$ F2	Muon identification	Forward Arm 2
eF2	Electron identification	Forward Arm 2
hF2	Hadron identification	Forward Arm 2

Configurations O and P add one Forward arm to N, resulting in the configuration featured in the BCD EOI.

Configurations Q and R instrument both Forward arms. Leaving out the muon system, as in case Q, lowers the cost but is not cost effective. Configuration R is the maximal case, and the most natural from the physics point of view.

In Table 12 we emphasize the physics that can be done with tracking and lepton identification, and begin with a minimal configuration, S, with only electron detection in a single Intermediate arm. Note that this configuration has a physics capability similar to that of the SFT.

Next we might expand either with muons in the Intermediate arm (T), or with electron in the Central region (U). Either step is equally effective in adding physics capability. Configuration V combines the additions of T and U.

A large increment of physics capability could be obtained by adding either the second Intermediate arm (W) or a Forward arm (X).

Configuration Y offers maximal lepton coverage, and we assess it with an overall figure of merit of  $2/3$  as  $\sin 2\varphi_3$  and  $B_s$  mixing have not been addressed.

Hadron identification could finally be added to reach configuration R of Table 12.

Configurations such as K or X that instrument only one are would be compatible with the installation of a gas-jet target upstream of the the interaction point on the free side, as suggested in EOI0013.

Table 12: Alternative detector configurations that maintain a broad-based *B*-physics program while expanding the solid-angle coverage. Refer to Table 11 for a description of the detector types. The acceptance for *B* physics is based on Table 7 of the BCD EOI, and is taken as the relative measure of the physics capability of each detector configuration. The cost estimate is based on Table 23 of the BCD EOI and includes contingency and EDIA of 40%. 'P/P' is a relative measure of performance/price and is proportional to Acc./Cost.

Config.	Detector															Acc.	Cost (\$M)	P/P
	$\mu$	$e$	$h$	$\mu$	$e$	$h$	$e$	$h$	$\mu$	$e$	$h$	$\mu$	$e$	$h$				
	F	F	F	I	I	I	C	C	I	I	I	F	F	F				
	1	1	1	1	1	1			2	2	2	2	2	2				
A							Y								0.004	66	0.07	
B							Y	Y							0.007	72	0.11	
C					Y	Y									0.006	81	0.09	
D				Y	Y	Y									0.012	98	0.14	
E	Y		Y												0.003	59	0.06	
F	Y	Y	Y												0.005	63	0.09	
G					Y	Y	Y	Y							0.031	109	0.33	
H				Y	Y	Y	Y	Y							0.055	126	0.50	
I		Y	Y		Y	Y									0.027	106	0.29	
J	Y	Y	Y	Y	Y	Y									0.053	133	0.46	
K		Y	Y	Y	Y	Y	Y	Y							0.080	155	0.59	
L	Y	Y	Y	Y	Y	Y	Y	Y							0.106	165	0.74	
M					Y	Y	Y	Y	Y	Y					0.079	160	0.57	
N				Y	Y	Y	Y	Y	Y	Y	Y				0.103	193	0.61	
O		Y	Y	Y	Y	Y	Y	Y	Y	Y	Y				0.131	200	0.75	
P	Y	Y	Y	Y	Y	Y	Y	Y	Y	Y	Y				0.154	208	0.85	
Q		Y	Y		Y	Y	Y	Y		Y	Y		Y	Y	0.102	182	0.65	
R	Y	Y	Y	Y	Y	Y	Y	Y	Y	Y	Y	Y	Y	Y	0.204	235	1	

## 5.2 Staging

Because of its modular design the BCD is readily staged. Referring to Table 12, a viable staging path for a broad physics capability would be configurations A - B - G - H - M - N - O - P - R, which builds up the detector symmetrically from the center. A path that builds up one arm first is also quite viable: A - B - G - H - K - L - R.

To begin with a good physics capability that includes study of  $\sin 2\varphi_3$ , it would be desirable to have at least configuration H as the initial implementation.

From Table 13 that emphasizes lepton identification, the staging paths might be S - T -

Table 13: Alternative detector configurations that specialize in reconstruction of  $B \rightarrow J/\psi K_S^0$  via emphasis on leptons. Refer to Table 11 for a description of the detector types. The acceptance for  $B$  physics is based on Table 7 of the BCD EOI, and is taken as the relative measure of the physics capability of each detector configuration. The cost estimate is based on Table 23 of the BCD EOI and includes contingency and EDIA of 40%. 'P/P' is a relative measure of performance/price and is proportional to Acc./Cost.

Config.	Detector															Acc.	Cost (\$M)	P/P
	$\mu$	$e$	$h$	$\mu$	$e$	$h$	$e$	$h$	$\mu$	$e$	$h$	$\mu$	$e$	$h$				
	F	F	F	I	I	I	C	C	I	I	I	F	F	F				
	1	1	1	1	1	1			2	2	2	2	2	2				
S					Y										0.005	52	0.05	
T				Y	Y										0.020	69	0.14	
U					Y		Y								0.020	67	0.14	
V				Y	Y		Y								0.035	83	0.20	
W				Y	Y		Y		Y	Y					0.080	95	0.40	
X	Y	Y		Y	Y		Y								0.090	121	0.35	
Y	Y	Y		Y	Y		Y		Y	Y		Y	Y		0.240	172	0.67	

V - W - Y - R, or S - U - V - X - Y - R. Configurations T, U, and even S already have very competitive capabilities for measurements of  $\sin 2\varphi_1$  and  $\sin 2\varphi_2$ .

We consider the mini-BCD to be an important stage towards BCD. It should measure  $B$ , mixing and provide evidence of  $CP$  violation if the latter is fairly strong.

## 6 Funding in FY91

6. The total funds requested in the EOI's for FY91 exceed the total funds available. It is assumed that most of the funds to be provided for detector R&D program will flow through the subsystem R&D program. For those funds requested in your EOI for systems integration and proposal preparation, please give a plan including a list of tasks in order of priority and with a detailed justification for each.

The BCD is involved in ongoing Subsystem R&D for silicon drift chambers, straw tube tracking, and online processor farms, which we expect will continue in FY91. In the BCD EOI (pp. 93-96) we proposed funding of four efforts, listed below, that will not be covered by Subsystem work but which are critical for determining the viability of proposed options for the BCD. We also now request funding to continue engineering support that began this Spring at the SSCL as part of the BCD contribution to the Resource Requirements Report.

The five items for which we seek funding are, in order of priority:

1. **Vertex Detector (\$520k).** We wish to pursue four issues of special relevance to the



---

BCD.

- a. C. Britton of ORNL has submitted to MOSIS an amplifier designed for the mini-BCD vertex detector. We request funds to submit this design to the rad-hard process of Harris Semiconductor, which would be the first use of this process in high-energy physics. Other high-energy groups would be welcome to join in this submission. (\$150k)
  - b. The BCD, Hughes Aircraft, U.C. Berkeley, LBL, and SLAC are participating in a Subsystem effort for pixel development. We wish to utilize Hughes' extensive systems engineering capabilities to evaluate a design of vertex detector optimized for physics of the BCD. This includes finite-element analysis of the mechanical design, heat-flow simulation, and evaluation of assembly and alignment techniques. Also, the BCD desires a readout system in which data from every event would be available to a local processor (the Hughes 3-D computer?) that could provide a secondary-vertex trigger. We solicit funding for Hughes to begin an engineering study of how such a scheme could be implemented, which effort would include design of relevant prototype readout chips. (\$200k)
  - c. U. Oklahoma and ORNL are now collaborating on radiation tests of silicon devices under the SSC Generic R&D Program. We propose to continue this work, but need new funding, as there is no BCD Subsystem program which could cover this need. (\$50k)
  - d. We wish to explore the fabrication of double-sided, AC-coupled detectors by a U.S.A. vendor, EG&G Reticon. At present no U.S.A. vendor makes such devices, but Reticon has expressed interests, and has demonstrated capability in silicon detectors. (\$120k)
2. **Time-of-Flight System (\$45k).** As discussed on pp. 61-62 of the BCD EOI, a high-performance time-of-flight system with resolution better than 90 psec might be sufficient to replace the RICH counters in the Central detector. Such performance has not yet been achieved, but is projected to be within reach by us and others (R. Stroynowski, private communication). Relatively modest funding could clarify this issue.
  3. **RICH Counters (\$155k).** Kaon identification in the Intermediate and Forward arms of the BCD must rely on RICH counters. These must operate at much higher rate than recent devices built for  $e^+e^-$  colliders. An R&D program should begin immediately to assess the viability of high-rate technology for the SSC. The work would be performed by the BCD in association with D. Anderson of Fermilab.
  4. **SSCL Engineering Support (2 engineers FTE).** Over the last few months the BCD has had excellent interaction with SSC engineers as part of the preparation of the Resource Requirements Report. We would like to continue this association in a formal manner to assist in system integration for the BCD Proposal.
  5. **Trigger Simulation (\$100k).** The BCD will rely on software triggers to a greater extent than is now common. It is important to begin a program of simulation of such

trigger scheme to validate this concept in a timely manner. We request support for two programmers, who would work with computers available at the SSCL and U. Penn.

## 7 References

- [1] *The Physics Program of a High-Luminosity Asymmetric B Factory at SLAC*, SLAC-353 (Oct. 1989).
- [2] D. Hitlin insisted we include this comparison in fairness to the  $e^+e^-$  options to show that they have nonzero capability to study  $\varphi_3$ .
- [3] E.L. Berger, *Benchmark Cross Sections for Bottom Quark Production*, Proceedings of the Workshop on High Sensitivity Beauty Physics at Fermilab, ed. by A.J. Slaughter, N. Lockyer, and M. Schmidt (Nov. 1987), p. 185; *Heavy Flavor Production*, ANL-HEP-PR 88-26 (1988).
- [4] I. Hinchliffe and M.D. Shapiro, *Report of the QCD Working Group*, Proceeding of the Summer Study on High Energy Physics in the 1990's, ed. by S. Jensen (Snowmass, 1988), p. 279; we use the average of the two curves shown in Fig. 4.
- [5] C. Albajar *et al.*, *Measurement of the Bottom Quark Production Cross Section in Proton-Antiproton Collisions at  $\sqrt{s} = 0.63$  TeV*, Phys. Lett. B213, 405 (1988).
- [6] M. Bauer, B. Stech, and M. Wirbel, *Exclusive Non-Leptonic Decays of D-, D<sub>s</sub>-, and B-Mesons*, Z. Phys. C 34, 103 (1987). The estimate of the branching ratio of  $B_s \rightarrow \rho^0 K_S^0$  as  $10^{-6}$  is taken from that for its exact analog  $B_d^0 \rightarrow \rho^0 \pi^0$ .
- [7] C. Haber has suggested that CDF could observe  $B_s$  mixing via partial reconstruction of leptonic decays; see M. Gold *et al.*, *B Physics with Existing Collider Detectors*, in Physics at Fermilab in the 1990's (Breckenridge, 1989), p. 247. We have not critically evaluated this difficult approach.
- [8] B. Campbell *et al.*, Phys. Rev. D 25, 1989 (1982).
- [9] A. Brandt *et al.*, *Study of Beauty Physics at the SPS-Collider with Real-Time Use of Silicon Microvertex Information*, CERN-SPSC/88-33 SPSC/P238; see section 4.2 of Addendum 1.